water

MDPI

Review

Advanced Oxidation Processes for Degradation of Water Pollutants—Ambivalent Impact of Carbonate Species: A Review

Manoj P. Rayaroth [1,*], Grzegorz Boczkaj [2,3], Olivier Aubry [1], Usha K. Aravind [4] and Charuvila T. Aravindakumar [5,6,*]

[1] Groupe de Recherches sur l'Energétique des Milieux Ionisés (GREMI), UMR 7344, Université d'Orléans, CNRS, 45067 Orléans, France
[2] Department of Sanitary Engineering, Faculty of Civil and Environmental Engineering, Gdansk University of Technology, G. Narutowicza 11/12 Str, 80-233 Gdansk, Poland
[3] EkoTech Center, Gdansk University of Technology, G. Narutowicza St. 11/12, 80-233 Gdansk, Poland
[4] School of Environmental Studies, Cochin University of Science & Technology (CUSAT), Kochi 682022, India
[5] School of Environmental Sciences, Mahatma Gandhi University, Kottayam 686560, India
[6] Inter University Instrumentation Centre, Mahatma Gandhi University, Kottayam 686560, India
* Correspondence: manoj.pr024@gmail.com (M.P.R.); cta@mgu.ac.in (C.T.A.)

Abstract: Advanced oxidation processes (AOPs) hold great promise in the removal of organic contaminants. Reactive oxygen species (ROS) produced in AOPs react with target pollutants to initially form several intermediate compounds that finally undergo complete mineralization. Such observations are reported, especially for laboratory-scale experiments performed in pure water. On the other hand, while considering real contaminated wastewater matrices, particularly industrial effluents, there are many co-existing ions. Carbonate ions are one of the major inorganic ions commonly existing in water resources. Hence, these ions have a significant impact on the respective water treatment processes. This review focused on the effect of carbonate ions on the degradation of pollutants in AOPs. In AOPs, carbonate radicals are formed by the scavenging reaction of the respective ions with ROS. The reactivity of these radicals towards the pollutant varies with respect to the structure and functionality. Therefore, depending on the functionalities of the contaminants, these ions show both positive and negative effects. Thus, this review aims to summarize the effects of carbonate species on the degradation of organic contaminants during AOPs and their environmental impacts. The carbonates enhanced the degradation of several emerging organic pollutants, including aniline, bisphenol A, rhodamine B, acid orange 7, naphthalene, and phenol derivatives. Carbonate presence was also revealed to have a positive contribution in cases of drug degradation, including sulfamethoxazole, propranolol, sulfamethazine, salbutamol, trimethoprim, azithromycin, naproxen, oxcarbazepine, and oxytetracycline.

Keywords: wastewater treatment; degradation mechanism; matrix effect; organic pollutants; scavenging; pharmaceuticals degradation

Citation: Rayaroth, M.P.; Boczkaj, G.; Aubry, O.; Aravind, U.K.; Aravindakumar, C.T. Advanced Oxidation Processes for Degradation of Water Pollutants—Ambivalent Impact of Carbonate Species: A Review. *Water* **2023**, *15*, 1615. https://doi.org/10.3390/w15081615

Academic Editors: Carmen Teodosiu, Yidi Chen and Florica Manea

Received: 21 March 2023
Revised: 6 April 2023
Accepted: 18 April 2023
Published: 20 April 2023

1. Introduction

Pollution of water resources by various organic chemicals has been identified as a growing crisis all over the world. The chemicals identified in the water sources are pesticides, pharmaceuticals, personal care products, dyes, volatile organic compounds, and many others. The importance of these pollutants is resistance towards biological action, malodor character, as well as persistence in the environment [1–7]. Even if they undergo different kinds of transformation or degradation, often the final product is likely to be more stable and toxic than the parent compound [8–10].

The degradation by means of highly reactive and non-selective oxygen species, mainly hydroxyl radicals (•OH), collectively called advanced oxidation processes (AOPs), is an

interesting area of research [11]. The degradation of contaminants and their derivatives by various AOPs, such as UV/H_2O_2 photolysis, photocatalysis, Fenton, electro-Fenton or cavitation-based methods, etc., resulted in good degradation and mineralization efficiency [11–16]. Moreover, there are other processes categorized in AOPs, such as the persulfate-mediated process, in which sulfate radical anions are the major species. Singlet oxygen also played a significant role in some AOPs [17–19]. When scaling up the process, researchers mainly addressed the operational parameters and operational pH, for example, light intensity in the case of light-mediated AOPs, such as photolysis, and photocatalysis, current density for electrochemical AOPs (EAOPs), and cavitation intensity in the case of cavitation-based AOPs and the concentration of the required oxidants. Moreover, there are other water matrices, more importantly, the co-existing ionic species that have a prominent role in any of the treatment techniques [20]. As a radical species-mediated process, these ions might have an impact on the removal efficiency [21–23].

When a real water matrix is considered, there are many inorganic ions, such as halide ions, sulfate ions, and carbonate and bicarbonate ions. All these ions affected the degradation efficiency aligned with competition kinetics with the reactive species. The effect can further be influenced by their concentration. In certain cases, the co-existing ions have a positive effect, if the secondary radical species had a high reactivity towards the pollutants and vice versa [23,24]. Carbonate species are the ions that contribute nearly 50% in all the water sources among the total ions. Therefore, this review has been made with the following objectives: (i) summarize the various sources of carbonate ions in water matrices, (ii) review the positive and negative impacts of carbonate ions in advanced oxidation processes and (iii) propose the suitable mechanism for the inhibition and promotion effect.

2. Carbonate Ions in Water Matrices

Carbonate species (CO_3^{2-}, and HCO_3^-) are the major component in the earth's crust and have significant importance in geological processes [25–27]. Carbonate-based rocks, such as limestone, dolomite, magnesite, chalk, and marble, are some of the natural forms of this ion and their minerals are present in the soil matrix [28–30]. Hence, soil erosion results in the generation of carbon dioxide (CO_2) and subsequent carbonation reaction with water releases carbonate or bicarbonate ions [31–33]. In addition, water passage through these rocks enhanced the dissolution of carbonates into the water [34,35]. Other important sources are the long-term deposition of the shells of fossilized snails, shellfish, and coral over millions of years [36]. The dissolution of CO_2 from the atmosphere also increases the carbonate concentration in the water matrix [37]. In addition, CO_2 is used as a feedstock for organic synthesis [38,39]. The unreactive CO_2 can be released into the aquatic matrix as respective ions.

Carbonate salt, especially $CaCO_3$, is widely used in building materials, paints, paper, and coating, and in the plastic industry as a filler and coating agent [40–42]. It is also used as an additive in the manufacturing of pesticides and poultry food [43]. As the daily application is considered, baking powder, toothpaste, detergents, agricultural lime, and animal feed contain these species [44]. Carbonic acid is the major ingredient in many soft drinks [45]. Sodium bicarbonate is used in fire extinguishers, in dyeing applications, and many other areas [46–48]. Hence, it is concluded that the concentration of CO_3^{2-} species in the water sources is huge. Even though these species are less toxic, their presence changes the pH of the water, and has an undesirable effect on the ecosystem. In addition, these species affect the removal efficiency of the water treatment processes. As an example, the carbonate precipitation results in fouling on the membrane surface, which further affects the removal efficiency [49]. However, a detailed analysis of their impact on AOP-based water purification technologies is very scarce. Hence, this review presents a comprehensive overview of the degradation and the transformation of pollutants in AOPs in the presence of carbonate species.

Speciation of carbonate species is given in Figure 1. It is clear that the major species in the acidic conditions are carbonic acid, bicarbonate ion in the neutral condition, and

carbonate ion in the alkaline condition [50]. Furthermore, in case of pH applicability of most of the AOPs, two forms always exist in the equilibrium. A specific case relates to pH 8, where mostly bicarbonate is present.

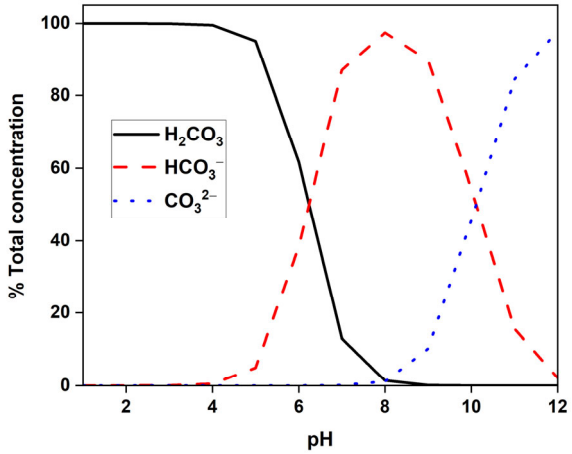

Figure 1. pH-dependent speciation of CO_3^{2-} species obtained from visual MINTEQ version 3.1, KTH, Sweden.

3. Carbonate Ions in AOPs

The major reactive species are $OH^\bullet$ in conventional AOPs and $SO_4^{\bullet-}$ in persulfate (PS)-based AOPs. Hence, the degradation depends on the bimolecular rate constant of reactive species with the target compound. Competition kinetics is proposed in co-existing matrices if they have a similar or higher bimolecular rate constant with the reactive species [21–23]. The $SO_4^{\bullet-}$ reacts with carbonate and bicarbonate ions with a bimolecular rate constant of 6.1×10^6 M^{-1} s^{-1} and 1.6×10^6 M^{-1} s^{-1}, respectively (Equations (1)–(5)) [51–53]. Even though the reaction kinetics for the reaction of $OH^\bullet$ and $SO_4^{\bullet-}$ towards HCO_3^- are similar, that for CO_3^{2-} with $OH^\bullet$ is 10^2 times higher than that with $SO_4^{\bullet-}$. Thus, the $OH^\bullet$ and $SO_4^{\bullet-}$ react with both CO_3^{2-} and HCO_3^- to form $CO_3^{\bullet-}$ as the major species. In comparison with $OH^\bullet$ and $SO_4^{\bullet-}$, $CO_3^{\bullet-}$ possesses lower redox potential (1.78 V) and high selectivity towards organic pollutants [54,55]. They have higher reactivity towards pollutants with electron-rich centers with bimolecular rate constant in the range of 10^3 to 10^9 $M^{-1}s^{-1}$ [56,57]. Hence, carbonate species show a dual effect in AOPs depending on the nature of the contaminants.

$$SO_4^{\bullet-} + CO_3^{2-} \rightarrow SO_4^{2-} + CO_3^{\bullet-}, \quad k = 6.1 \times 10^6\ M^{-1}\ s^{-1} \tag{1}$$

$$SO_4^{\bullet-} + HCO_3^- \rightarrow SO_4^{2-} + HCO_3^{\bullet}, \quad k = 1.6 \times 10^6\ M^{-1}\ s^{-1} \tag{2}$$

$$OH^\bullet + CO_3^{2-} \rightarrow OH^- + CO_3^{\bullet-}, \quad k = 3.9 \times 10^8\ M^{-1}\ s^{-1} \tag{3}$$

$$OH^\bullet + HCO_3^- \rightarrow OH^- + HCO_3^{\bullet}, \quad k = 1.6 \times 10^6\ M^{-1}\ s^{-1} \tag{4}$$

$$HCO_3^{\bullet} \leftrightarrow H^+ + CO_3^{\bullet-} \tag{5}$$

The highly selective nature of the $CO_3^{\bullet-}$ makes it more selective towards electron-rich moieties such as -NH_2, -OH (especially phenols), and aromatic rings. $CO_3^{\bullet-}$ accept an electron from the electron-rich center to form radical cations. The release of the H atom from this species and a subsequent rearrangement forms a carbon-centered radical [54,58]. The H abstraction can also form a carbon-centered radical. An attack of carbonate radical on

these transient species and the release of bicarbonate ions forms the hydroxylated product (Figure 2).

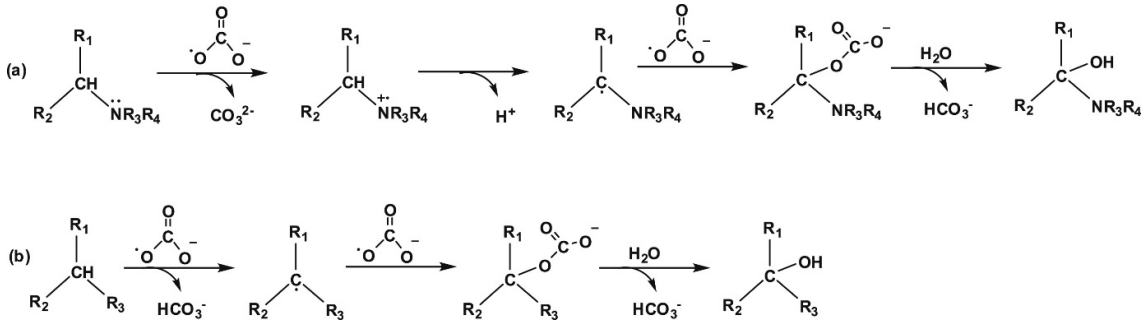

Figure 2. Hydroxylation by an electron transfer (**a**) and hydrogen abstraction (**b**) mechanism initiated by $CO_3^{\bullet-}$. Reprinted with permission from [58].

4. Enhancement of Degradation Efficiency by Carbonate Radical

As described in the previous sections, there are many reactions or changes taking place in the carbonate solution containing reactive species. The positive effect of carbonate is reported if the compound bears some characteristic functional groups, such as substituted phenols, naphthalene ring derivatives, aniline derivatives, etc. This further depends on the concentration of the $CO_3^{\bullet-}$ formed in the medium. Studies reporting the improved degradation of pollutants by carbonate species in AOPs are given in Table 1. The experimental conditions, including the concentration of pollutants and bicarbonates, are given in this table. In general, the concentration of the pollutants in water sources are detected in the range of microgram per liter to milligram per liter [59,60]. However, the concentration of pollutants in the selected studies are higher than their normal concentration in contaminated water sources and most of the studies are conducted in pure water. This selection is compiled to study the exact degradation behavior in the presence of co-existing matrices and to identify the intermediate products.

The effect of HCO_3^- in UV/H_2O_2 photolysis for a set of pharmaceuticals is presented in Figure 3. It is obvious that the effect of $^{\bullet}OH$ is completely masked by the HCO_3^- ions in some cases and secondary radicals are contributing to the degradation in the latter cases. The negative effect is mainly attributed by the scavenging effect and the low reactivity of the resulting secondary species towards the pollutant and vice versa [61]. The bimolecular rate constant for the reaction of $CO_3^{\bullet-}$ with some micropollutants are given in Table 2.

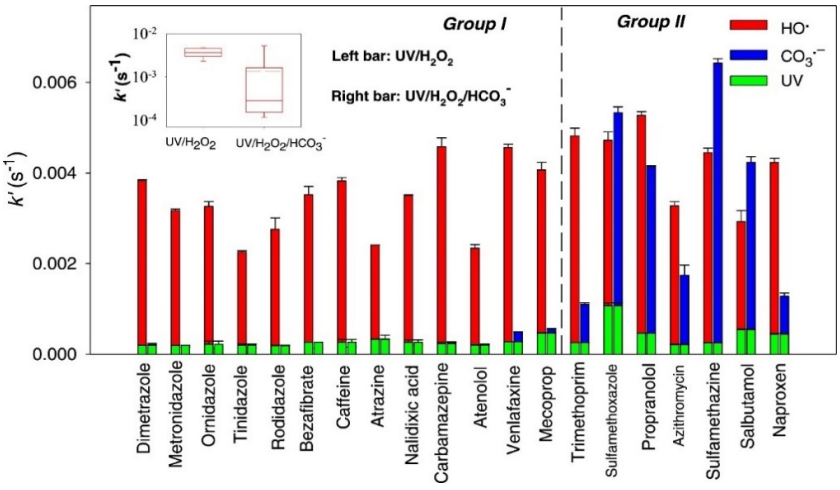

Figure 3. The effect of CO_3^{2-} on the rate of degradation of various pharmaceutical pollutants using the UV/H_2O_2 photolysis method. Reprinted with permission from [61].

Table 1. The list of pollutants showing an improvement in the degradation in AOPs combined with carbonate species.

AOPs	Pollutant	Experimental Conditions	Positive Effect	Ref.
		Sonolysis		
Sonolysis	Triphenyl methane dyes (TPM)	$[C]_0$ = 10 ppm, $[CO_3^{2-}]$ = 10–100 ppm, Freq = 350 kHz, applied input power 60 W	The degradation of ethyl violet and Coomassie brilliant blue was decreased and that of pararosaniline was increased.	[62]
Sonolysis	Bisphenol A (BPA)	$[C]_0$ = 0.12 µM; Freq = 300 kHz; Power; 80 W; pH 8.3; $[HCO_3^-]$ = 500 mgL^{-1} T = 21 °C	60% degradation in 5 min without HCO_3^- and increased to 98% with HCO_3^-	[63]
Sonolysis	Rhodamine B (RhB)	$[C]_0$ = 0.5 mg L^{-1}; $[HCO_3^-]$ = 3 g L^{-1}; temperature: 25 °C; pH: 8.3; frequency: 300 kHz; power: 60 W.	Degradation efficiency increased from 60% to 99% in 20 min with HCO_3^- addition.	[64]
Sonolysis	Naphthol blue black (NBB)	$[C]_0$ = 8.1 µM Frequency: 278 kHz, Power: 100 W, Volume: 400 mL, Temperature: 20 ± 1 °C, $NaHCO_3$: 2.97 mM.	The degradation of NBB is not affected even in the presence of nonyl phenol by carbonate addition	[65]
		UV/Oxidants		
UV/H_2O_2 UV/PS UV/NH_2Cl UV/Cl_2	Naproxen (NPX)	$[C]_0$ = 5 µM, $[Oxidant]_0$ = 50 µM, $[HCO_3^-]_0$ = 50 mM.	The production of $CO_3^{\bullet-}$ was more and hence the degradation in UV/NH_2Cl	[61]
UV/H_2O_2	Oxcarbazepine (OXC)	$[C]_0$ = 10 µM, $[H_2O_2]_0$ = 500 µM, $[HCO_3^-]_0$ = 10 mM, pH = 8.0,	Three times increase in the degradation rate.	[66]
UV/H_2O_2 UV/PS	Oxytetracycline (OTC)	$[C]_0$ = 10 µM, $[H_2O_2]_0$ = PS = 1 mM, $[CO_3^{2-}]$ = 2 mM	Increased the degradation in both oxidation systems	[67]
		Activated PS (peroxydisulfate (PDS) and peroxymonosulfate (PMS))		
Heat activated PS	SMX	$[C]_0$ = 30 µM, $[PDS]_0$ = 2 mM, $[HCO_3^-]_0$ = 0–20 mM, T = 50 °C,	Degradation increased from 50% to 99% with HCO_3- ions	[68]
Heat activated PS	SMZ	$[C]_0$ = 30 µM, $[PDS]_0$ = 2.0 mM, $[HCO_3^-]_0$ = 50 mM, T = 50 °C,	Complete degradation within 120 min	[69]
Ce(III)/PMS	Naphthalene derivatives	$[C]_0$ = $[Ce(III)]_0$ = 5.0 mmol L^{-1}, $[PMS]_0$ = 5.0 mmol L^{-1}; $[HCO_3^-]_0$ = 500 mg L^{-1},	Positive effect was reported for napthalene, methyl and nitro derivatives.	[70]
$CuFe_2O_4$/PMS	BPA	$[C]_0$ = 50 mg L^{-1}; $[PMS]_0$ = 0.5 mM; $[CuFe_2O_4]$ = 0.5 g L^{-1}, $[HCO_3^-]_0$ = 0.1 M	99% dégradation within 15 min.	[71]
CuS/PMS	4-methyl Phenols (4-MP)	$[C]_0$ = 0.08 mmol/L, $[PMS]_0$ = 0.2 g/L, [CuS] = 0.15 g/L, $[CO_3^{2-}]_0$ = 2 mmol/L	80% of 4-MP was degraded with CuS/PMS in 5 min. Complete degradation within 2 min in the presence of carbonate ions.	[72]
		Photocatalysis		
$CuO_x/BiVO_4$	BPA	$[C]_0$ = 210 µg/L; 0.75 Cu/BVO, $[HCO_3^-]_0$ = 500 mg/L	10 times increase in the degradation rate was observed with the bicarbonate addition.	[73]
UV/TiO_2	Aniline	$[C]_0$ = 5 × 10^{-3} mol dm^{-3}, $[TiO_2]$ = 0.86 g/L, $[Na_2CO_3]_0$ = 0.1 M	Lower concentration (0.11 M) increased the degradation rate.	[74]
UV/TiO_2	Cylindrospermopsin (CYN)	$[C]_0$ = 10 µM, $[TiO_2]$ = 0.25 g/L, $[Na_2CO_3]_0$ = 1.5 mM	Not affected the degradation but decreased the by-product formation.	[58]

Table 1. *Cont.*

AOPs	Pollutant	Experimental Conditions	Positive Effect	Ref.
		EAOPs		
BDD anode/SS cathode	naphthenic acids (NAs)	Oil sands process water (OSPW), Current density, 30 mA cm^{-2}	100% COD removal in 2 h.	[75]
PbO2/SS/Graphite cathode	Methyl Orange	$[C]_0$ = 50 mgL^{-1}, Current density = 2.87 mA cm^{-2}, [NaCl] = 1 g L^{-1} $[Na_2CO_3]_0$ = 300 mgL^{-1}	Degradation rate increased from 0.0126 min^{-1} to 0.0141 min^{-1}	[76]
Ti/SnO2-Sb/Ce-PbO2/SS cathode	Lamivudine	$[C]_0$ = 5 mgL^{-1}, Current density = 10 mA cm^{-2}, $[Na_2SO_4]$ = 20 mM $[Na_2CO_3]_0$ = 50 mM	Degradation rate increased from 1.34 min^{-1} to 14.53 min^{-1}	[77]
Carbon fiber anode/graphite cathode	Phenol	$[C]_0$ = 0.1 mM, Current density = 0.06 mA cm^{-2}, $[NaHO_3]_0$ = 50 mM	Complete degradation within 2 h.	[78]
		Oxidant activation by carbonate species		
PMS/CO_3^{2-}	BPA	$[C]_0$ = 0.05 mM, $[CO_3^{2-}]_0$ = 5 mM, and $[PMS]_0$ = 1 mM.	Complete degradation was observed within 40 min. The degradation rate increased from 0.02 min^{-1} to 0.12 min^{-1} with increase in pH from 3 to 11.	[79]
HCO_3^-/PS	Acetaminophen	$[C]_0$ = 10 µM; $[HCO_3^-]_0$ = 25 mM, $[PS]_0$ = 10 mM, pH 8.3.	75% degradation after 7 h.	[80]
CO_3^{2-}/H_2O_2	Acid orange 7	$[C]_0$ = 0.2 mM, $[CO_3^{2-}]_0$ = 10 mM, $[H_2O_2]_0$ = 5 mM	90% degradation in 6 h.	[81]
CO_3^{2-}/PMS	SMX	$[C]_0$ = 10 mg/L, $[PMS]_0$ = 1 mM, $[CO_3^{2-}]_0$ = 5 mM	Complete degradation within 3 h.	[82]
CO_3^{2-}/PMS	Acid orange 7	$[C]_0$ = 0.05 mM, $[PMS]_0$ = 1 mM, $[CO_3^{2-}]_0$ = 5 mM	The rate of degradation increased from 0.0006 to 0.1342 min^{-1} with an increase in CO_3^{2-} to 5 mM.	[83]

Table 2. The bimolecular rate constants for the reaction of $CO_3^{\bullet-}$ with some pharmaceuticals [61].

Pollutant	Bimolecular Rate Constant, k $CO_3^{\bullet-}$ ($M^{-1}s^{-1}$)
Salbutamol	1.51×10^8 $M^{-1}s^{-1}$
Paracetamol	1.70×10^8 $M^{-1}s^{-1}$
Vanillic acid	5.0×10^8 $M^{-1}s^{-1}$
p-coumaric acid	4.60×10^8 $M^{-1}s^{-1}$
Propranolol	1.92×10^8 $M^{-1}s^{-1}$
Naproxen (NPX)	5.60×10^7 $M^{-1}s^{-1}$
Sulfamethoxazole (SMX)	2.48×10^8 $M^{-1}s^{-1}$
Sulfamethazine (SMZ)	2.96×10^8 $M^{-1}s^{-1}$
Clenbuterol	5.20×10^8 $M^{-1}s^{-1}$
Diclofenac	7.80×10^7 $M^{-1}s^{-1}$

Table 2. *Cont.*

Pollutant	Bimolecular Rate Constant, k $CO_3^{\bullet-}$ ($M^{-1}s^{-1}$)
Sotalol	2.20×10^8 $M^{-1}s^{-1}$
Trimethoprim	4.91×10^7 $M^{-1}s^{-1}$
Carbamazepine	1.25×10^7 $M^{-1}s^{-1}$)
Atenolol	9.79×10^6 $M^{-1}s^{-1}$
Nitroimidazoles	$5.09–9.11 \times 10^6$ $M^{-1}s^{-1}$
Atrazine	9.39×10^6 $M^{-1}s^{-1}$
Nalidixic acid	7.49×10^6 $M^{-1}s^{-1}$
Caffeine	6.09×10^6 $M^{-1}s^{-1}$
Azithromycin	9.12×10^7 $M^{-1}s^{-1}$
Erythromycin A	8.0×10^7 $M^{-1}s^{-1}$
Bezafibrate	5.33×10^6 $M^{-1}s^{-1}$
Gemfibrozil	4.10×10^6 $M^{-1}s^{-1}$
Clofibric acid	1.0×10^7 $M^{-1}s^{-1}$

5. UV Coupled with Oxidants

Activation of external oxidants added into the treated medium by UV light is effective in the generation of ROS and the rapid degradation of variety of contaminants [84]. In this process, the photoirradiation can break the peroxobond (-O-O-) in the oxidants, such as H_2O_2, persulfates, and ozone (Equation (6)) [84–87]. Other oxidants, such as hydroxyl amine and chlorine, are also used in UV-based AOPs [24].

$$\text{-O-O- + h}\nu \rightarrow \text{Reactive species} \quad (6)$$

The degradation of 20 PPCPs by UV/H_2O_2 photolysis was studied by Zhou et al. The PPCPs were degraded effectively with a rate constant range of 0.00225–0.00527 s^{-1}. The carbonate ions had a positive effect depending on the structure of the compound. The addition of 50 mM of HCO_3^- significantly increased the degradation of pollutants such as sulfamethoxazole, sulfamethazine, and salbutamol [61]. By comparing the specific reaction rate constants of reactive species, such as $^{\bullet}OH$ and $CO_3^{\bullet-}$, the $^{\bullet}OH$ is completely "masked" and $CO_3^{\bullet-}$ becomes prominent for those pollutants. In addition, they have compared the impact of HCO_3^- in other UV-oxidants, such as H_2O_2, PS, Cl_2, and NH_2Cl. Among these oxidants, a significant improvement in the degradation of NPX was observed in UV/NH_2Cl [24]. In this system, reactive nitrogen species (RNS) are involved in addition to other reactive oxygen and chlorine species. All these species except the $ClO^{\bullet}$ react with the CO_3^{2-} (*k:* 600 $M^{-1}s^{-1}$). The reported concentration of $CO_3^{\bullet-}$ in the UV/H_2O_2, UV/Cl_2, UV/NH_2Cl and UV/PS were 2.2×10^{-11}, 9.5×10^{-10}, 5.2×10^{-9} M, and 6.8×10^{-11} M, respectively. Hence, even though $CO_3^{\bullet-}$ possesses lower reactivity towards NPX, their high concentration and longer lifetime enable effective degradation [24].

Liu et al. investigated the transformation of oxytetracycline in the UV/H_2O_2 system in carbonate solution. The degradation was promoted with the addition of CO_3^{2-}. In UV/H_2O_2 photolysis, the rate constant was 4.8×10^{-3} cm^2 mJ^{-1}, which is increased to 6×10^{-3} cm^2 mJ^{-1} with the increase in CO_3^{2-}/HCO_3^- concentration. The pH change increases the electron density around the compound and facilitates the reaction of carbonate radical. Furthermore, the role of carbonate radicals in UV/NO_3^-, UV/H_2O_2, and UV/PS oxidation processes was investigated for oxytetracycline degradation. The degradation efficiency for oxytetracycline in UV/NO_3^- was 30%, and that in UV/H_2O_2 was 90% with UV fluence of 320 mJ/cm^2. However, the 90% degradation was observed with a lower UV

fluence of 80 mJ/cm^2 in the UV/PS process. The addition of NO_3^- had a negligible effect in both UV/oxidant systems. On the other hand, adding HCO_3^- had a positive effect in all the above UV-activated systems. Moreover, the UV/PS was also revealed to be effective in natural water [67].

6. Activated Persulfate (PS)

Persulfates (PS, both peroxydisulfate (PDS) and peroxymonosulfate (PMS)) are widely used oxidants in the removal of organic pollutants from both water and soil matrices. This oxidant itself can oxidize the pollutants directly due to their oxidation potential of 2.07 V [88,89]. However, the direct oxidation of the pollutants is limited to certain organics with electron-rich centers, such as -NH_2, sulfur containing moieties, etc. However, the mineralization rate is slow in this process due to the stability of the intermediate compounds. The rate of reaction and mineralization in the PS process is enhanced by certain activators [90–92]. Because of the activators, such as light source, heat, and cavitation, many catalysts can break the O-O bond in PS to produce $SO_4^{\bullet-}$ and $^\bullet$OH. Other reactive species, such as $O_2^{\bullet-}$ and $^1O_2$ are formed based on the interaction between the catalysts and PS (Equation (7)) [91,92]. Carbon-based materials, Fe-based materials, single-atom catalysts, etc., are commonly used in the generation of other reactive species than $SO_4^{\bullet-}$ and $^\bullet$OH [93–95].

$$\text{PS (PMS or PDS)} + \text{activators} \rightarrow SO_4^{\bullet-}, {}^\bullet OH, O_2^{\bullet-}, \text{and } {}^1O_2 \quad (7)$$

A study conducted by Chen et al. compared the degradation efficiencies of various naphthalene derivatives (naphthalene, -CH_3 (1-MN), -NO_2 (1-NN), -OH (1-NAP), -NH_2 (1-NA)) using Ce(III)/PMS. The degradation rates of NAP, 1-MN, 1-NN in Ce(III)/PMS, were 0.0080, 0.0086, 0.0119, and it was increased to 0.0131 min^{-1} for NAP, 0.0096 min^{-1} for 1-MN, and 0.0133 min^{-1} for 1-NN. The results indicate that the functional groups, such as –NO_2 and –CH_3 attached to NAP, improved the degradation efficiency through their effect on the charge distribution of NAP derivatives [70]. Another study was conducted with different phenols with functional groups, such as isopropyl, methyl, methoxy, dimethyl, amino, chloro, carboxylic acid, and nitro in CuS/PMS/CO_3^{2-} systems. Among these derivatives, phenol with electron-donating groups, such as isopropyl, methyl, methoxy, and amino groups, undergo faster degradation compared to phenol in the presence of CO_3^{2-} and vice versa [72].

In some cases, the changes in the pH by the addition of carbonate ions influence the zero-point charge (pzc) of the catalyst. The PS activation is affected by such changes. A positive effect was reported in the sludge-activated carbon-based $CoFe_2O_4$ activated PMS system for norfloxacin degradation. This is the fact at lower concentrations of CO_3^{2-} [96].

7. Cavitation Process

In cavitation processes, microbubbles are formed in the liquid medium induced by the vibrational motion. The bubble size gets increased in each cycle and finally undergoes adiabatic bubble collapse (implosion). Under these conditions hot spot regions are formed, providing a perfect environment for the formation of the reactive radical species ($^\bullet$H and $^\bullet$OH) (Equation (8)) [97–102]. In addition, the pollutants undergo thermal degradation with respect to their physicochemical properties (hydrophilicity or hydrophobicity). The ionic effect in the cavitation process is affected through the salting out mechanism. If the ions caused the salting out of the pollutants towards the reactive regime, cavitating bubbles, it enables thermal and oxidation.

$$H_2O))))) \rightarrow H^\bullet + {}^\bullet OH \quad (8)$$

Sonochemical degradation of various dyes in the triphenyl methane (TPM) category was already reported [62,103]. More than 98% degradation of ethyl violet (EV) and pararosaniline (PRA) was achieved under sonochemical conditions of 350 kHz and 60 W

input power. Among these two dyes, an increased degradation was reported in the case of PRA. A nearly 3-fold increase in the degradation rate was observed in this case [62]. On the other hand, the degradation of Coomassie brilliant blue is not affected by the carbonate or bicarbonate ions [103]. The TPM dyes are degraded via hydroxylation, de-alkylation, and bond cleavage of the central carbon atom. These ions also affected some of the by-product formations. The presence of carbonate ions reduced the formation of hydroxylated products and enhanced the destruction of conjugated structures in the molecule. As can be seen from Figure 4, carbonate radicals speed up the formation of carbon-centered radical (II). For RhB, an increase in the bicarbonate concentration from 0.1 to 3 g/L enhanced the degradation efficiency. Moreover, the effect becomes visible at lower concentrations of the RhB [64]. Similar results, i.e., an enhancement in the degradation at lower pollutant concentrations, was reported for bisphenol S, N,N-Diethyl-meta-toluamide (DEET), 4-cumylphenol, etc. [104–106].

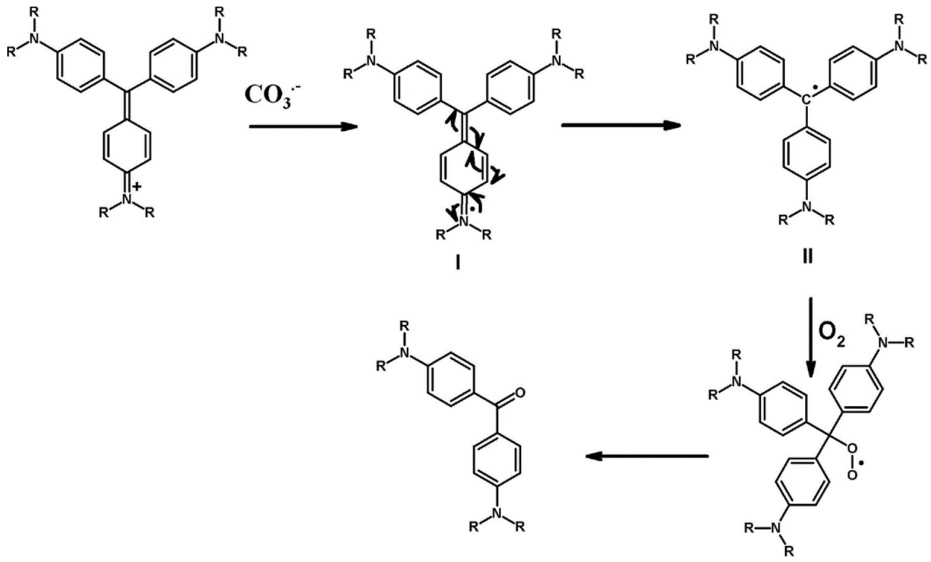

Figure 4. The destruction of TPM dyes induced by $CO_3^{\bullet -}$. Reprinted with permission from [62].

As mentioned in the previous sections, a visible enhancement is attained at a lower BPA concentration. Sonolysis of 0.12 µM of BPA resulted a 60% degradation in pure water (0.025 µmol min^{-1} L^{-1}). An increase in bicarbonate concentration from 12 to 500 mg/L (0.05 µmol min^{-1} L^{-1}) caused the complete degradation of BPA in 5 min [63]. In the case of sono-Fenton reaction with copper film, the carbonate ions inhibited the degradation. Further addition of the ions increased the degradation but did not reach the control reaction [107].

8. Photocatalysis

In photocatalysis, reactive species are formed by photoirradiation on the photocatalytic surface. Electron-hole pairs are formed initially, and the hole reacts with the water to generate $^{\bullet}OH$. The reduction in O_2 by the electron forms $O_2^{\bullet -}$ (Equations (9)–(11)) [108,109]. The effect of carbonate ions in photocatalysis is mainly through the scavenging of the reactive species and the surface properties of the material.

$$TiO_2 + h\nu \rightarrow h_{VB}^{+} + e^{-}_{CB} \quad (9)$$

$$h_{VB}^{+} + (H_2O)_{ads} \rightarrow {}^{\bullet}OH \quad (10)$$

$$e^{-}_{CB} + O_2 \rightarrow O_2^{\bullet -} \quad (11)$$

The degradation of aniline in TiO_2 photocatalysis was increased with the addition of CO_3^{2-} species. The rate of degradation in photocatalysis was 2.7×10^{-6} and is increased to 6.5×10^{-6} mol dm^{-3} s^{-1} with the addition of 0.1 M Na_2CO_3. The carbonate ions also affected the product formation. Azobenzene and nitrobenzene are the major intermediates formed in the photocatalytic oxidation of aniline in the presence of carbonate ions. On the other hand, nitrobenzene was not detected in pure photocatalytic system [74]. A similar tendency was reported for CYN and hexylpyridinium bromide (HPyBr). The number of intermediates detected in the presence of carbonate ions was less than that detected in the pure photocatalytic process, especially sulfate group elimination byproducts [58]. An enhancement effect was reported for anthraquinone (AQ) during the photocatalytic degradation with faceted TiO_2. In this case, the rate of degradation was increased from 0.0089 min^{-1} to 0.0109 min^{-1} in the presence of 100 mgL^{-1} bicarbonate ion. The intensity of EPR signals for $^{\bullet}OH$ is decreased with the increase in HCO_3^- concentration. It indicates the strong scavenging of $^{\bullet}OH$ by HCO_3^- [110].

Another possibility in photocatalysis is the interaction of the photocatalytic surface with carbonate ions. In the TiO_2–CO_3^{2-} system, the CO_3^{2-} ion bonds with TiO_2 through the oxygen atom at alkaline pH and supplements a site for the adsorption of contaminants (Figure 5). This interaction may stabilize the suspension. The oxidation of carbonate ions by the hole acts as an additional source for carbonate radicals in the medium [110].

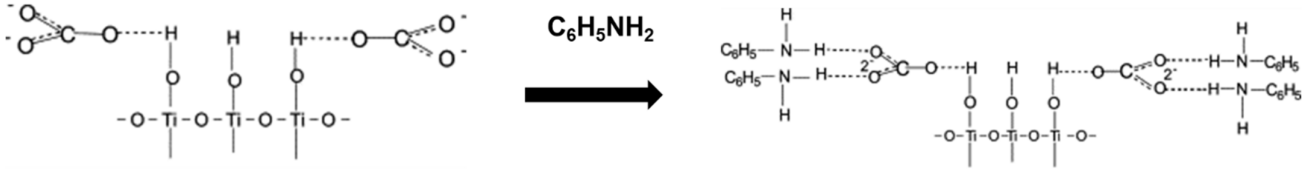

Figure 5. Adsorption of aniline on the surface of carbonate-modified TiO_2.

9. Electrochemical Advanced Oxidation Processes (EAOPs)

EAOPs are another important technique in AOPs, which have been widely used in the rapid mineralisation of organic compounds from various water matrices [111,112]. Anodic (direct) oxidation and the indirect oxidation by the in situ generated oxidants are the two major pathways involved in this process (Equations (12) and (13)). In the first pathway, the pollutants are degraded either by the direct electron transfer or the by the $^{\bullet}OH$ on the anodic surface. In indirect process, the reactive species are formed in the solution by the reaction of in situ generated oxidants, especially H_2O_2 by the electrochemical reactions depending on the anode materials or electrolyte [113].

$$M + H_2O \rightarrow M(^{\bullet}OH) + {}^{-}OH + e^- \quad (12)$$

$$M(^{\bullet}OH) \rightarrow MO + H^+ + e^- \quad (13)$$

As the major species in EAOPs are $^{\bullet}OH$, the scavenging reactions and the subsequent formation of $CO_3^{\bullet-}$ are possible, such as other AOPs. Compared to other AOPs, there are extra sources of $CO_3^{\bullet-}$ during the electrochemical oxidation of solution containing carbonate species. It has been reported that the carbonate species undergo direct reaction at the anode, especially on the 'nonactive' boron doped diamond (BDD) anode (Equations (14)–(20)) [75]. The carbon fibre electrode produced more hydrogen peroxide compared to graphite electrode and led to the rapid transformation of carbonate ions to respective reactive species, peroxy-monocarbonate ions [78]. Min et al. compared the degradation of phenol by graphite anode carbon fibre anode in a carbonate electrolyte solution. It has been found that the complete degradation of phenol occurs in 2 h with a carbon fibre anode, whereas complete degradation was not achieved even after 4 h with a graphite anode [78]. This difference is mainly attributed to the larger surface area of the material.

Ganiu et al. studied the degradation of naphthenic acids (NAs) and their derivatives, in oil sands process water (OSPW) [75]. Complete degradation of these contaminants has been observed in 2 h with a current density of 30 mA cm^{-2}. The process generated $CO_3^{\bullet-}$ when the electrolyte is carbonate medium as clear from the electron paramagnetic resonance (EPR) data. Non radical species, $C_2O_6^{2-}$ were also formed at a concentration of 2 mM during the reaction.

Pillai et al. compared the effect of carbonate and bicarbonate ions on the degradation of methyl orange, malachite green and 2,4-dinitrophenol by EAOPs. Among the three pollutants, only methyl orange showed the positive effect in carbonate ion medium [76].

Brito et al. studied the degradation of rifampicin under various electrolyte mediums with BDD/carbon felt electrochemical systems. The COD is enhanced in the presence of carbonate ions, nearly reaching 95% reduction owing to the formation of both radical and non-radical species [114]. Wang et al. found a positive effect of bicarbonate ions during the degradation of a drug, lamivudine using Ti/SnO_2-Sb/Ce-PbO_2. The rate of degradation was increased from 1.3×10^{-1} to 14.5×10^{-1} min^{-1}, with an increase in HCO_3^- concentration from 0 to 50 mM [77].

$$CO_3^{2-} \rightarrow CO_3^{\bullet-} + e^- \quad (14)$$

$$M(OH^{\bullet}) + CO_3^{2-} \rightarrow M + CO_3^{\bullet-} + OH^-, \quad (15)$$

$$2\,M(OH^{\bullet}) + 2HCO_3^- \rightarrow 2M + C_2O_6^{2-} + H_2O, \quad (16)$$

$$2\,CO_3^{2-} \rightarrow C_2O_6^{2-} + 2\,e^-, \quad (17)$$

$$2\,CO_3^{\bullet-} \rightarrow C_2O_6^{2-} \quad (18)$$

$$C_2O_6^{2-} + H_2O \rightarrow 2\,CO_3^{2-} + H_2O_2 + 2H^+ \quad (19)$$

$$HCO_3^- + H_2O_2 \rightarrow HCO_4^- \quad (20)$$

10. Activation of Oxidants by Carbonate Species

An important aspect of carbonate species in oxidant-mediated AOPs (H_2O_2, and PDS) is their influence on oxidant stability. Carbonate ions are normally inert towards these oxidants, but the bicarbonate reacts with the oxidants to form strong percarbonates. On the other hand, PMS is reactive toward both the carbonate species to form ROS and percarbonates (Equations (21)–(25)). The decomposition of oxidants is further influenced by the change in the pH (to alkaline), which can activate the oxidants to form ROS, such as $OH^{\bullet}$ and $SO_4^{\bullet-}$, $O_2^{\bullet-}$, and $^1O_2$ (Figure 6) [24].

$$HCO_3^- + H_2O_2 \rightarrow HCO_4^- + H_2O \quad (21)$$

$$HCO_3^- + S_2O_8^{2-} + 2OH^- \rightarrow HCO_4^- + 2SO_4^{2-} + H_2O \quad (22)$$

$$CO_3^{2-} + HSO_5^- + H^+ \rightarrow SO_4^{\bullet-} + 2OH^- + CO_2 \quad (23)$$

$$HCO_3^- + HSO_5^- \rightarrow SO_4^{\bullet-} + 2OH^- + CO_2 \quad (24)$$

$$HCO_3^- + HSO_5^- \rightarrow SO_4^{2-} + HCO_4^- + H^+ \quad (25)$$

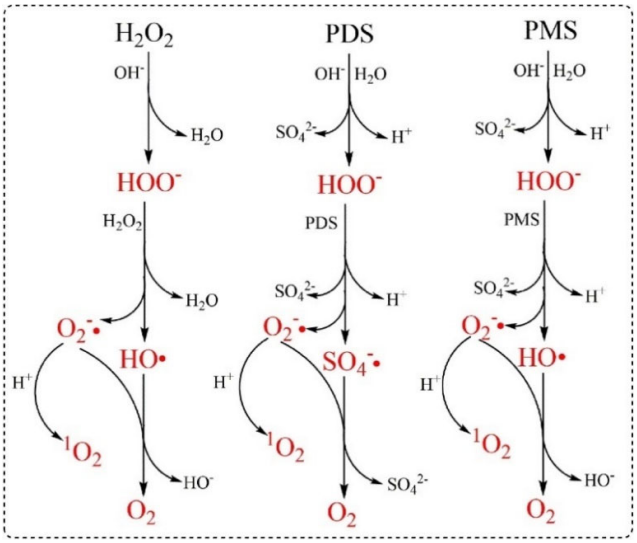

Figure 6. The dissociation of oxidants by the addition of carbonate species and the subsequent generation of ROS. Reprinted with permission from [24].

Sun et al. reported an enhancement in the degradation of SMX by PMS in the presence of carbonate ions. Complete degradation of SMX was reported in this study, and 20% of TOC removal was achieved compared to the process with PMS alone. Nearly 30% of the PMS was decomposed in the system with CO_3^{2-}, PMS, and SMX [82]. Nie et al., also utilized the same process for the degradation of acid orange 7 (AO7). A complete degradation of AO7 within 40 min was achieved by this process. A pH range of 3–9 was effective for this process, and inhibition was observed beyond this range. An appreciable removal was observed for other pollutants, such as methylene blue, acetaminophen, phenol, methyl orange, and para-aminobenzoic acid. The scavenging experiment in the presence of alcohols ($^{\bullet}OH$ and $SO_4^{\bullet-}$), L-histidine, and sodium azide ($^1O_2$) shows that the major reactive species are $^1O_2$, which enhanced the degradation [83]. PS activated by HCO_3^- was reported to be effective in the degradation of acetaminophen, but the process takes place relatively slowly. Nearly 7 h was required to achieve 60% removal [80].

Li et al. used CO_3^{2-} as an activator of H_2O_2 in the degradation of an azo dye, acid orange 7 (AO7). Nearly 83% degradation was reported after 8 h at an initial pH of 12. The degradation was increased from 0 to more than 90% by increasing the concentration of H_2O_2 from 0 to 50 mM at a fixed CO_3^{2-} concentration of 10 mM. A scavenging experiment with methanol and tert-butanol shows an insignificant effect on the degradation, indicating a negligible effect of $^{\bullet}OH$. However, the para-benzoquinone and ascorbic acid had a prominent effect on the degradation. It indicates that the superoxide radical is strongly involved in the process. The super oxide radical can be converted into $^1O_2$ [81].

11. Inhibitory Effect of Carbonate Ions

There are many studies reporting the inhibitory effect of carbonate species in AOPs due to the scavenging of reactive species ($^{\bullet}OH$ or $SO_4^{\bullet-}$). Hence, some selected studies are presented in this section.

The inhibitory effect is reported when the $CO_3^{\bullet-}$ shows lower reactivity towards the contaminants. Wang et al. reported the negative effect of HCO_3^- during the degradation of bisphenol S (BPS) by heat-activated PS. BPS undergoes nearly 76% degradation in 3 h by this process in pure water. The addition of 50 mM HCO_3^- reduced the degradation efficiency to 53%. Compared to other inorganic species, the effect is more prominent [115]. A similar effect is reported for other pharmaceuticals, such as simazine, losartan, carbamazepine, thiamethoxam, etc., [116–120]. Liu et al. reported the negative effect of HCO_3^- in the soil remediation of BPA by PS activated with biochar [121]. The efficiency of PS activation by zerovalent iron (ZVI)-based materials are strongly retarded by the presence

of carbonate species. A complete degradation of 50 µM benzoic acid within 60 min without any interfering species has been found. However, the addition of 50 mM of CO_3^{2-} ions completely masked the degradation. The similar effect is reported for both ZVI and sulfide-modified ZVI [122]. The addition of carbonate ions reduced the sonochemical degradation of many pollutants. The degradation of methyl paraben reduced to 80% from 100% in 90 min with the addition of 100 ppm of carbonate ions [123]. A similar effect is reported for pollutants such as coomassie brilliant blue, crystal violet, penicillinic antibiotics, propyl paraben, ethyl paraben, neonicotinoid, etc. [103,124–127].

Tan et al. compared the effect of carbonate species in various UV-based AOPs for the degradation of antipyrine. The rate constant for the degradation in the UV system without HCO_3^- addition was 1.455 ± 0.005 h^{-1}. A slight decrease in the rate to 1.4 h^{-1} was observed with the addition of 200 mM HCO_3^-. In the UV/H_2O_2 system, the rate constant was 1.99 h^{-1}, and it was decreased to 1.27 h^{-1} in the presence of this ion. On the other hand, rate constants of 1.65 and 1.54 h^{-1} were observed with and without the addition of HCO_3^- in the UV/PS system [128]. A similar effect is reported for parathion, florfenicol, thiamphenicol, losartan potassium, furosemide, caffeine, carbendazim, anatoxin, propranolol, acetaminophen in UV-based oxidation treatments [129–131].

In photocatalysis, these inorganic species sometimes adsorb on the catalytic surface and block the active site. Moreover, it can affect the photocatalytic efficiency by the scavenging effect. The degradation of phenol by ZnO photocatalysis showed a strong inhibition effect in the presence of carbonate ions. Phenol underwent 78% during the 4-h photo irradiation of ZnO catalyst. In this case, CO_3^{2-} scavenges both hole and $^{\bullet}OH$ and hence reduces the formation of reactive species in the medium. Another chance is the effect of these species on the pzc of the photocatalyst by changing the solution pH. The pzc of ZnO is 8.7–9.2. The carbonate ions at a higher concentration increased the pH to 10. Hence, the charge of ZnO becomes negative. It repelled the negatively charged pollutant from the catalyst surface and decreased the removal efficiency [132]. The reduction in the efficiency of this kind of AOP is reported for pollutants, such as phenanthrene, naphthalene, BTEX, phenolic compounds, dichloroethane, parabens, etc. [133–136].

As in the case of other AOPs, the scavenging happens in the liquid medium in EAOPs with the addition of carbonate species. Additionally, electrochemical reactions of these species can also affect the removal efficiency. The rate constant for the COD removal from malachite green solution by EO using BDD anode was 0.0086 min^{-1}, and it was decreased to 0.0042 min^{-1} with the addition of 500 ppm carbonate species [76]. In the case of an antibiotic, norfloxacin using IrO_2 anodes in various matrices, such as municipal wastewater, urine, and seawater, showed that the carbonate species is the major species in retarding the degradation efficiency [137]. In this case, 70% of the degradation in 20 min was attained in NaCl, which is reduced to 3% with the addition of HCO_3^- ions. A similar inhibitory effect is reported with Ti–IrO_2 mixed-metal oxide anode during the degradation of atrazine isoproturon, carbamazepine, metoprolol, and atenolol [138]. Another effect of carbonate species in EAOP is the scaling of $CaCO_3$ on the cathodic surface, which reduced the oxidation effect. This is reported in the case of ciprofloxacin and sulfamethoxazole in the real wastewater samples [139].

12. Conclusions and Future Recommendations

AOPs are effective in the removal of various organic contaminants with a high mineralization rate. However, the efficiency of the processes is highly dependent on the nature of the contaminant sources. The co-existing water matrix, especially the inorganic anions, is one of the critical factors that affect the efficiency of AOPs. Carbonate ions are one of the major inorganic species present in the water matrix, which strongly scavenges the reactive species involved in AOPs. Their presence often reduces degradation efficiency. Even though the secondary radical, $CO_3^{\bullet-}$, did not generate toxic intermediates, such as halide ions, it had a significant effect on the concentration of the intermediates and

subsequently the removal of toxicity. Hence detailed product monitoring is an important step in the carbonate abundant water sources.

This review shows that carbonate species affected the degradation of organic contaminants in AOPs. The contaminants with electron-donating moieties, such as isopropyl, methyl, methoxy, and amino, exhibit improved degradation in the presence of carbonates. Detailed profiling of the water samples for the presence of carbonate species or the respective contaminants before implementing a treatment method is obviously needed to fully understand the degradation mechanism and the influence of matrix effects.

Activation of oxidants, especially PMS, can be adapted in the carbonate abundant matrix. The carbonate/PMS process generates many reactive oxygen species, including $^1O_2$, which allows for contaminant degradation in real case scenario. However, a high concentration of the carbonate ions retarded the process as well. Hence, an optimization of carbonate concentration is required. By continuing this research, another oxidant formed from sodium carbonate and H_2O_2, sodium percarbonate, is currently widely explored.

In carbonate-mediated AOPs, selective reactive species, such as $CO_3^{\bullet-}$ and $^1O_2$, are generated. Hence, it has shown a positive effect on various compounds in the category of drugs, dyes, and many other emerging contaminants. The degradation in each case further depends on the structural properties, especially the functional groups present in it. In several cases, it is clear that increased degradation can be obtained using carbonates that are naturally present in the real aqueous matrix. Focus on this aspect providing lowered costs of treatment and lowered consumption of oxidants falls into the idea of sustainable development and should be further explored.

13. Methodology

A thorough literature search has been done on various sources, such as Scopus, web of science, and google scholar. The keywords selected in searching the literature were "*advanced oxidation, pollutants, degradation, carbonate ions*", "*advanced oxidation, pollutants, degradation, inorganic ions*", "*sonolysis, pollutants, carbonate ions*", "*carbonate radicals, pollutants, degradation*", and "*electrochemical oxidation, pollutants, degradation, carbonate ions*". To cover most of the topics on the promotion effect, we have collected literature throughout the year. However, for the inhibitory effect, a paper published in the last 10–15 years was selected, and only important data are provided.

Author Contributions: Conceptualization, M.P.R.; Investigation, M.P.R.; Writing—Original Draft Preparation, M.P.R.; Writing—Review and Editing, G.B.; Writing—Review and Editing, O.A.; Writing—Review and Editing, U.K.A.; Supervision, C.T.A. All authors have read and agreed to the published version of the manuscript.

Funding: This research was funded by [Centre Val de Loire] grant number [APR IR #2021-00144786].

Data Availability Statement: The data presented in this study are available on request from the corresponding author.

Conflicts of Interest: The authors declare no competing interest.

References

1. Petrie, B.; Barden, R.; Kasprzyk-Hordern, B. A review on emerging contaminants in wastewaters and the environment: Current knowledge, understudied areas and recommendations for future monitoring. *Water Res.* **2015**, *72*, 3–27. [CrossRef] [PubMed]
2. Philip, J.M.; Aravind, U.K.; Aravindakumar, C.T. Emerging contaminants in Indian environmental matrices—A review. *Chemosphere* **2018**, *190*, 307–326. [CrossRef] [PubMed]
3. La Farré, M.; Pérez, S.; Kantiani, L.; Barceló, D. Fate and toxicity of emerging pollutants, their metabolites and transformation products in the aquatic environment. *TrAC Trends Anal. Chem.* **2008**, *27*, 991–1007. [CrossRef]
4. Edelstein, M.; Ben-Hur, M. Heavy metals and metalloids: Sources, risks and strategies to reduce their accumulation in horticultural crops. *Sci. Hortic.* **2018**, *234*, 431–444. [CrossRef]
5. Chowdhury, P.; Viraraghavan, T. Sonochemical degradation of chlorinated organic compounds, phenolic compounds and organic dyes—A review. *Sci. Total. Environ.* **2009**, *407*, 2474–2492. [CrossRef]

6. Chow, R.; Scheidegger, R.; Doppler, T.; Dietzel, A.; Fenicia, F.; Stamm, C. A review of long-term pesticide monitoring studies to assess surface water quality trends. *Water Res. X* **2020**, *9*, 100064. [CrossRef]
7. Fernandes, A.; Gągol, M.; Makoś, P.; Khan, J.A.; Boczkaj, G. Integrated photocatalytic advanced oxidation system (TiO2/UV/O3/H2O2) for degradation of volatile organic compounds. *Sep. Purif. Technol.* **2019**, *224*, 1–14. [CrossRef]
8. El-Shahawi, M.; Hamza, A.; Bashammakh, A.; Al-Saggaf, W. An overview on the accumulation, distribution, transformations, toxicity and analytical methods for the monitoring of persistent organic pollutants. *Talanta* **2010**, *80*, 1587–1597. [CrossRef]
9. Lipczynska-Kochany, E. Humic substances, their microbial interactions and effects on biological transformations of organic pollutants in water and soil: A review. *Chemosphere* **2018**, *202*, 420–437. [CrossRef]
10. Barber, L.B.; Keefe, S.H.; Brown, G.K.; Furlong, E.T.; Gray, J.L.; Kolpin, D.W.; Meyer, M.T.; Sandstrom, M.W.; Zaugg, S.D. Persistence and Potential Effects of Complex Organic Contaminant Mixtures in Wastewater-Impacted Streams. *Environ. Sci. Technol.* **2013**, *47*, 2177–2188. [CrossRef]
11. Rayaroth, M.P.; Marchel, M.; Boczkaj, G. Advanced oxidation processes for the removal of mono and polycyclic aromatic hydrocarbons—A review. *Sci. Total. Environ.* **2023**, *857*, 159043. [CrossRef] [PubMed]
12. Wang, J.L.; Xu, L.J. Advanced Oxidation Processes for Wastewater Treatment: Formation of Hydroxyl Radical and Application. *Crit. Rev. Environ. Sci. Technol.* **2012**, *42*, 251–325. [CrossRef]
13. Pignatello, J.J.; Oliveros, E.; Mackay, A. Advanced Oxidation Processes for Organic Contaminant Destruction Based on the Fenton Reaction and Related Chemistry. *Crit. Rev. Environ. Sci. Technol.* **2006**, *36*, 1–84. [CrossRef]
14. Boczkaj, G.; Fernandes, A. Wastewater treatment by means of advanced oxidation processes at basic pH conditions: A review. *Chem. Eng. J.* **2017**, *320*, 608–633. [CrossRef]
15. Fernandes, A.; Makoś, P.; Khan, J.A.; Boczkaj, G. Pilot scale degradation study of 16 selected volatile organic compounds by hydroxyl and sulfate radical based advanced oxidation processes. *J. Clean. Prod.* **2019**, *208*, 54–64. [CrossRef]
16. Rayaroth, M.P.; Aravindakumar, C.T.; Shah, N.S.; Boczkaj, G. Advanced oxidation processes (AOPs) based wastewater treatment-unexpected nitration side reactions—A serious environmental issue: A review. *Chem. Eng. J.* **2022**, *430*, 133002. [CrossRef]
17. Domingues, E.; Silva, M.J.; Vaz, T.; Gomes, J.; Martins, R.C. Sulfate radical based advanced oxidation processes for agro-industrial effluents treatment: A comparative review with Fenton's peroxidation. *Sci. Total. Environ.* **2022**, *832*, 155029. [CrossRef]
18. Duan, X.; Yang, S.; Wacławek, S.; Fang, G.; Xiao, R.; Dionysiou, D.D. Limitations and prospects of sulfate-radical based advanced oxidation processes. *J. Environ. Chem. Eng.* **2020**, *8*, 103849. [CrossRef]
19. Rayaroth, M.P.; Prasanthkumar, K.P.; Kang, Y.-G.; Lee, C.-S.; Chang, Y.-S. Degradation of carbamazepine by singlet oxygen from sulfidized nanoscale zero-valent iron–citric acid system. *Chem. Eng. J.* **2020**, *382*, 122828. [CrossRef]
20. Stefan, M.I. (Ed.) *Advanced Oxidation Processes for Water Treatment: Fundamentals and Applications*; IWA Publishing: London, UK, 2017. [CrossRef]
21. Yang, Y.; Pignatello, J.J.; Ma, J.; Mitch, W.A. Comparison of Halide Impacts on the Efficiency of Contaminant Degradation by Sulfate and Hydroxyl Radical-Based Advanced Oxidation Processes (AOPs). *Environ. Sci. Technol.* **2014**, *48*, 2344–2351. [CrossRef]
22. Tufail, A.; Price, W.E.; Hai, F.I. A critical review on advanced oxidation processes for the removal of trace organic contaminants: A voyage from individual to integrated processes. *Chemosphere* **2020**, *260*, 127460. [CrossRef] [PubMed]
23. Ribeiro, A.R.L.; Moreira, N.F.; Puma, G.L.; Silva, A.M. Impact of water matrix on the removal of micropollutants by advanced oxidation technologies. *Chem. Eng. J.* **2019**, *363*, 155–173. [CrossRef]
24. Wang, J.; Wang, S. Effect of inorganic anions on the performance of advanced oxidation processes for degradation of organic contaminants. *Chem. Eng. J.* **2021**, *411*, 128392. [CrossRef]
25. Zhan, N.; Huang, Y.; Rao, Z.; Zhao, X.-L. Fast Detection of Carbonate and Bicarbonate in Groundwater and Lake Water by Coupled Ion Selective Electrode. *Chin. J. Anal. Chem.* **2016**, *44*, 355–360. [CrossRef]
26. Desmarais, K.; Rojstaczer, S. Inferring source waters from measurements of carbonate spring response to storms. *J. Hydrol.* **2002**, *260*, 118–134. [CrossRef]
27. Sappa, G.; Ergul, S.; Ferranti, F. Water quality assessment of carbonate aquifers in southern Latium region, Central Italy: A case study for irrigation and drinking purposes. *Appl. Water Sci.* **2014**, *4*, 115–128. [CrossRef]
28. Kumar, A.; Kumar Tripathi, V.; Sachan, P.; Rakshit, A.; Singh, R.M.; Shukla, S.K.; Pandey, R.; Vishwakarma, A.; Panda, K.C. Chapter 10—Sources of ions in the river ecosystem. In *Ecological Significance of River Ecosystems*; Madhav, S., Kanhaiya, S., Srivastav, A., Singh, V., Singh, P., Eds.; Elsevier: Amsterdam, The Netherlands, 2022; pp. 187–202. [CrossRef]
29. Sharma, S.; Bhattacharya, A. Drinking water contamination and treatment techniques. *Appl. Water Sci.* **2017**, *7*, 1043–1067. [CrossRef]
30. Morse, J.W.; Arvidson, R.S. The dissolution kinetics of major sedimentary carbonate minerals. *Earth Sci. Rev.* **2002**, *58*, 51–84. [CrossRef]
31. Connor, R. *The United Nations World Water Development Report 2015: Water for a Sustainable World*; UNESCO Publishing: Paris, France, 2015.
32. Alghobar, M.A.; Suresha, S. Evaluation of Nutrients and Trace Metals and Their Enrichment Factors in Soil and Sugarcane Crop Irrigated with Wastewater. *J. Geosci. Environ. Prot.* **2015**, *3*, 46–56. [CrossRef]
33. Kim, J.H.; Jobbágy, E.G.; Richter, D.D.; Trumbore, S.E.; Jackson, R.B. Agricultural acceleration of soil carbonate weathering. *Glob. Chang. Biol.* **2020**, *26*, 5988–6002. [CrossRef]
34. Schlesinger, W.H. An evaluation of abiotic carbon sinks in deserts. *Glob. Chang. Biol.* **2017**, *23*, 25–27. [CrossRef] [PubMed]

35. Wang, C.; Li, W.; Yang, Z.; Chen, Y.; Shao, W.; Ji, J. An invisible soil acidification: Critical role of soil carbonate and its impact on heavy metal bioavailability. *Sci. Rep.* **2015**, *5*, 12735. [CrossRef] [PubMed]
36. Boyjoo, Y.; Pareek, V.K.; Liu, J. Synthesis of micro and nano-sized calcium carbonate particles and their applications. *J. Mater. Chem. A* **2014**, *2*, 14270–14288. [CrossRef]
37. Daschakraborty, S.; Kiefer, P.M.; Miller, Y.; Motro, Y.; Pines, D.; Pines, E.; Hynes, J.T. Reaction Mechanism for Direct Proton Transfer from Carbonic Acid to a Strong Base in Aqueous Solution I: Acid and Base Coordinate and Charge Dynamics. *J. Phys. Chem. B* **2016**, *120*, 2271–2280. [CrossRef]
38. Zhang, D.; Xue, Y.; Zheng, X.; Zhang, C.; Li, Y. Multi-heterointerfaces for selective and efficient urea production. *Natl. Sci. Rev.* **2023**, *10*, nwac209. [CrossRef]
39. Liu, Q.; Wu, L.; Jackstell, R.; Beller, M. Using carbon dioxide as a building block in organic synthesis. *Nat. Commun.* **2015**, *6*, 5933. [CrossRef]
40. Saulat, H.; Cao, M.; Khan, M.M.; Khan, M.; Rehman, A. Preparation and applications of calcium carbonate whisker with a special focus on construction materials. *Constr. Build. Mater.* **2020**, *236*, 117613. [CrossRef]
41. Betancourt, D.; Martirena, F.; Day, R.; Diaz, Y. The influence of the addition of calcium carbonate on the energy efficiency of fired clay bricks manufacture. *Rev. Ing. Constr.* **2007**, *22*, 187–196.
42. Ali, M.; Abdullah, M.S.; Saad, S.A. Effect of Calcium Carbonate Replacement on Workability and Mechanical Strength of Portland Cement Concrete. *Adv. Mater. Res.* **2015**, *1115*, 137–141. [CrossRef]
43. Niu, Y.-Q.; Liu, J.-H.; Aymonier, C.; Fermani, S.; Kralj, D.; Falini, G.; Zhou, C.-H. Calcium carbonate: Controlled synthesis, surface functionalization, and nanostructured materials. *Chem. Soc. Rev.* **2022**, *51*, 7883–7943. [CrossRef]
44. Fu, J.; Leo, C.P.; Show, P.L. Recent advances in the synthesis and applications of pH-responsive CaCO3. *Biochem. Eng. J.* **2022**, *187*, 108446. [CrossRef]
45. Tahmassebi, J.; Duggal, M.; Malik-Kotru, G.; Curzon, M. Soft drinks and dental health: A review of the current literature. *J. Dent.* **2006**, *34*, 2–11. [CrossRef] [PubMed]
46. Ramalingam, S.; Jonnalagadda, R.R. Tailoring Nanostructured Dyes for Auxiliary Free Sustainable Leather Dyeing Application. *ACS Sustain. Chem. Eng.* **2017**, *5*, 5537–5549. [CrossRef]
47. Chang, C.-Y.; Wu, P.-H.; Hsiao, C.-T.; Chang, C.-P.; Chen, Y.-C.; Wu, K.-H. Sodium bicarbonate administration during in-hospital pediatric cardiac arrest: A systematic review and meta-analysis. *Resuscitation* **2021**, *162*, 188–197. [CrossRef]
48. Fahmi, A.; Ahmadi, R.; Memar, M.Y.; Hemmati, S.; Babakhani, S.; Samadi-Kafil, H.; Katebi, H.; Haghighatara, S. A novel microbial-assisted method for sodium bicarbonate production—Cleaner production, safe and facile synthesis. *Process. Saf. Environ. Prot.* **2022**, *163*, 694–702. [CrossRef]
49. Mikhaylin, S.; Bazinet, L. Fouling on ion-exchange membranes: Classification, characterization and strategies of prevention and control. *Adv. Colloid Interface Sci.* **2016**, *229*, 34–56. [CrossRef]
50. Epedersen, O.; Colmer, T.D.; Esand-Jensen, K. Underwater Photosynthesis of Submerged Plants—Recent Advances and Methods. *Front. Plant Sci.* **2013**, *4*, 140. [CrossRef]
51. Buxton, G.V.; Elliot, A.J. Rate constant for reaction of hydroxyl radicals with bicarbonate ions. *Int. J. Radiat. Appl. Instrum. Part C. Radiat. Phys. Chem.* **1986**, *27*, 241–243. [CrossRef]
52. Huie, R.E.; Clifton, C.L. Temperature dependence of the rate constants for reactions of the sulfate radical, SO4-, with anions. *J. Phys. Chem.* **1990**, *94*, 8561–8567. [CrossRef]
53. Mertens, R.; von Sonntag, C. Photolysis (λ = 354 nm of tetrachloroethene in aqueous solutions. *J. Photochem. Photobiol. A Chem.* **1995**, *85*, 1–9. [CrossRef]
54. Neta, P.; Huie, R.E.; Ross, A.B. Rate Constants for Reactions of Inorganic Radicals in Aqueous Solution. *J. Phys. Chem. Ref. Data* **1988**, *17*, 1027–1284. [CrossRef]
55. Burg, A.; Shamir, D.; Shusterman, I.; Kornweitz, H.; Meyerstein, D. The role of carbonate as a catalyst of Fenton-like reactions in AOP processes: $CO_3^{\cdot-}$ as the active intermediate. *Chem. Commun.* **2014**, *50*, 13096–13099. [CrossRef] [PubMed]
56. Moore, J.; Phillips, G.; Sosnowski, A. Reaction of the Carbonate Radical Anion with Substituted Phenols. *Int. J. Radiat. Biol. Relat. Stud. Phys. Chem. Med.* **1977**, *31*, 603–605. [CrossRef]
57. Wols, B.; Harmsen, D.; Wanders-Dijk, J.; Beerendonk, E.; Hofman-Caris, C. Degradation of pharmaceuticals in UV (LP)/H2O2 reactors simulated by means of kinetic modeling and computational fluid dynamics (CFD). *Water Res.* **2015**, *75*, 11–24. [CrossRef] [PubMed]
58. Zhang, G.; He, X.; Nadagouda, M.N.; O'Shea, K.E.; Dionysiou, D.D. The effect of basic pH and carbonate ion on the mechanism of photocatalytic destruction of cylindrospermopsin. *Water Res.* **2015**, *73*, 353–361. [CrossRef]
59. Kumar, R.; Qureshi, M.; Vishwakarma, D.K.; Al-Ansari, N.; Kuriqi, A.; Elbeltagi, A.; Saraswat, A. A review on emerging water contaminants and the application of sustainable removal technologies. *Case Stud. Chem. Environ. Eng.* **2022**, *6*, 100219. [CrossRef]
60. Patel, M.; Kumar, R.; Kishor, K.; Mlsna, T.; Pittman, C.U., Jr.; Mohan, D. Pharmaceuticals of Emerging Concern in Aquatic Systems: Chemistry, Occurrence, Effects, and Removal Methods. *Chem. Rev.* **2019**, *119*, 3510–3673. [CrossRef]
61. Zhou, Y.; Chen, C.; Guo, K.; Wu, Z.; Wang, L.; Hua, Z.; Fang, J. Kinetics and pathways of the degradation of PPCPs by carbonate radicals in advanced oxidation processes. *Water Res.* **2020**, *185*, 116231. [CrossRef]
62. Rayaroth, M.P.; Aravind, U.K.; Aravindakumar, C.T. Effect of inorganic ions on the ultrasound initiated degradation and product formation of triphenylmethane dyes. *Ultrason. Sonochem.* **2018**, *48*, 482–491. [CrossRef]

63. Pétrier, C.; Torres-Palma, R.; Combet, E.; Sarantakos, G.; Baup, S.; Pulgarin, C. Enhanced sonochemical degradation of bisphenol-A by bicarbonate ions. *Ultrason. Sonochem.* **2010**, *17*, 111–115. [CrossRef]
64. Merouani, S.; Hamdaoui, O.; Saoudi, F.; Chiha, M.; Pétrier, C. Influence of bicarbonate and carbonate ions on sonochemical degradation of Rhodamine B in aqueous phase. *J. Hazard. Mater.* **2010**, *175*, 593–599. [CrossRef] [PubMed]
65. Dalhatou, S.; Laminsi, S.; Pétrier, C.; Baup, S. Competition in sonochemical degradation of Naphthol Blue Black: Presence of an organic (nonylphenol) and a mineral (bicarbonate ions) matrix. *J. Environ. Chem. Eng.* **2019**, *7*, 102819. [CrossRef]
66. Liu, T.; Yin, K.; Liu, C.; Luo, J.; Crittenden, J.; Zhang, W.; Luo, S.; He, Q.; Deng, Y.; Liu, H.; et al. The role of reactive oxygen species and carbonate radical in oxcarbazepine degradation via UV, UV/H2O2: Kinetics, mechanisms and toxicity evaluation. *Water Res.* **2018**, *147*, 204–213. [CrossRef]
67. Liu, Y.; He, X.; Duan, X.; Fu, Y.; Fatta-Kassinos, D.; Dionysiou, D.D. Significant role of UV and carbonate radical on the degradation of oxytetracycline in UV-AOPs: Kinetics and mechanism. *Water Res.* **2016**, *95*, 195–204. [CrossRef] [PubMed]
68. Ji, Y.; Fan, Y.; Liu, K.; Kong, D.; Lu, J. Thermo activated persulfate oxidation of antibiotic sulfamethoxazole and structurally related compounds. *Water Res.* **2015**, *87*, 1–9. [CrossRef]
69. Fan, Y.; Ji, Y.; Kong, D.; Lu, J.; Zhou, Q. Kinetic and mechanistic investigations of the degradation of sulfamethazine in heat-activated persulfate oxidation process. *J. Hazard. Mater.* **2015**, *300*, 39–47. [CrossRef]
70. Chen, X.; Wang, P.; Peng, F.; Zhou, Z.; Waigi, M.G.; Ling, W. Ce(III) activates peroxymonosulfate for the degradation of substituted PAHs. *Chemosphere* **2022**, *306*, 135525. [CrossRef]
71. Xu, Y.; Ai, J.; Zhang, H. The mechanism of degradation of bisphenol A using the magnetically separable CuFe2O4/peroxymonosulfate heterogeneous oxidation process. *J. Hazard. Mater.* **2016**, *309*, 87–96. [CrossRef]
72. Wang, X.; Zhou, Y.; Wang, N.; Zhang, J.; Zhu, L. Carbonate-induced enhancement of phenols degradation in CuS/peroxymonosulfate system: A clear correlation between this enhancement and electronic effects of phenols substituents. *J. Environ. Sci.* **2023**, *129*, 139–151. [CrossRef]
73. Kanigaridou, Y.; Petala, A.; Frontistis, Z.; Antonopoulou, M.; Solakidou, M.; Konstantinou, I.; Deligiannakis, Y.; Mantzavinos, D.; Kondarides, D.I. Solar photocatalytic degradation of bisphenol A with CuO x /BiVO 4: Insights into the unexpectedly favorable effect of bicarbonates. *Chem. Eng. J.* **2017**, *318*, 39–49. [CrossRef]
74. Kumar, A.; Mathur, N. Photocatalytic degradation of aniline at the interface of TiO2 suspensions containing carbonate ions. *J. Colloid Interface Sci.* **2006**, *300*, 244–252. [CrossRef]
75. Ganiyu, S.O.; El-Din, M.G. Insight into in-situ radical and non-radical oxidative degradation of organic compounds in complex real matrix during electrooxidation with boron doped diamond electrode: A case study of oil sands process water treatment. *Appl. Catal. B Environ.* **2020**, *279*, 119366. [CrossRef]
76. Pillai, I.M.S.; Gupta, A.K. Effect of inorganic anions and oxidizing agents on electrochemical oxidation of methyl orange, malachite green and 2,4-dinitrophenol. *J. Electroanal. Chem.* **2016**, *762*, 66–72. [CrossRef]
77. Wang, Y.; Zhou, C.; Chen, J.; Fu, Z.; Niu, J. Bicarbonate enhancing electrochemical degradation of antiviral drug lamivudine in aqueous solution. *J. Electroanal. Chem.* **2019**, *848*, 113314. [CrossRef]
78. Min, S.-J.; Kim, J.-G.; Baek, K. Role of carbon fiber electrodes and carbonate electrolytes in electrochemical phenol oxidation. *J. Hazard. Mater.* **2020**, *400*, 123083. [CrossRef] [PubMed]
79. Abdul, L.; Si, X.; Sun, K.; Si, Y. Degradation of bisphenol A in aqueous environment using peroxymonosulfate activated with carbonate: Performance, possible pathway, and mechanism. *J. Environ. Chem. Eng.* **2021**, *9*, 105419. [CrossRef]
80. Jiang, M.; Lu, J.; Ji, Y.; Kong, D. Bicarbonate-activated persulfate oxidation of acetaminophen. *Water Res.* **2017**, *116*, 324–331. [CrossRef]
81. Li, Y.; Li, L.; Chen, Z.-X.; Zhang, J.; Gong, L.; Wang, Y.-X.; Zhao, H.-Q.; Mu, Y. Carbonate-activated hydrogen peroxide oxidation process for azo dye decolorization: Process, kinetics, and mechanisms. *Chemosphere* **2018**, *192*, 372–378. [CrossRef] [PubMed]
82. Sun, Y.; Xie, H.; Zhou, C.; Wu, Y.; Pu, M.; Niu, J. The role of carbonate in sulfamethoxazole degradation by peroxymonosulfate without catalyst and the generation of carbonate racial. *J. Hazard. Mater.* **2020**, *398*, 122827. [CrossRef]
83. Nie, M.; Zhang, W.; Yan, C.; Xu, W.; Wu, L.; Ye, Y.; Hu, Y.; Dong, W. Enhanced removal of organic contaminants in water by the combination of peroxymonosulfate and carbonate. *Sci. Total. Environ.* **2019**, *647*, 734–743. [CrossRef] [PubMed]
84. Li, W.; Jain, T.; Ishida, K.; Liu, H. A mechanistic understanding of the degradation of trace organic contaminants by UV/hydrogen peroxide, UV/persulfate and UV/free chlorine for water reuse. *Environ. Sci. Water Res. Technol.* **2017**, *3*, 128–138. [CrossRef]
85. Kim, I.; Yamashita, N.; Tanaka, H. Photodegradation of pharmaceuticals and personal care products during UV and UV/H2O2 treatments. *Chemosphere* **2009**, *77*, 518–525. [CrossRef]
86. Peyton, G.R.; Glaze, W.H. Destruction of pollutants in water with ozone in combination with ultraviolet radiation. 3. Photolysis of aqueous ozone. *Environ. Sci. Technol.* **1988**, *22*, 761–767. [CrossRef] [PubMed]
87. Thomas, N.; Dionysiou, D.D.; Pillai, S.C. Heterogeneous Fenton catalysts: A review of recent advances. *J. Hazard. Mater.* **2021**, *404*, 124082. [CrossRef]
88. Kolthoff, I.M.; Miller, I.K. The Chemistry of Persulfate. I. The Kinetics and Mechanism of the Decomposition of the Persulfate Ion in Aqueous Medium[1]. *J. Am. Chem. Soc.* **1951**, *73*, 3055–3059. [CrossRef]
89. Wang, J.; Wang, S. Activation of persulfate (PS) and peroxymonosulfate (PMS) and application for the degradation of emerging contaminants. *Chem. Eng. J.* **2018**, *334*, 1502–1517. [CrossRef]

90. Honarmandrad, Z.; Sun, X.; Wang, Z.; Naushad, M.; Boczkaj, G. Activated persulfate and peroxymonosulfate based advanced oxidation processes (AOPs) for antibiotics degradation—A review. *Water Resour. Ind.* **2023**, *29*, 100194. [CrossRef]
91. Zhang, B.-T.; Zhang, Y.; Teng, Y.; Fan, M. Sulfate Radical and Its Application in Decontamination Technologies. *Crit. Rev. Environ. Sci. Technol.* **2015**, *45*, 1756–1800. [CrossRef]
92. Zhou, Z.; Liu, X.; Sun, K.; Lin, C.; Ma, J.; He, M.; Ouyang, W. Persulfate-based advanced oxidation processes (AOPs) for organic-contaminated soil remediation: A review. *Chem. Eng. J.* **2019**, *372*, 836–851. [CrossRef]
93. Fang, Y.; Liu, Y.; Qi, L.; Xue, Y.; Li, Y. 2D graphdiyne: An emerging carbon material. *Chem. Soc. Rev.* **2022**, *51*, 2681–2709. [CrossRef]
94. Xue, Y.; Huang, B.; Yi, Y.; Guo, Y.; Zuo, Z.; Li, Y.; Jia, Z.; Liu, H.; Li, Y. Anchoring zero valence single atoms of nickel and iron on graphdiyne for hydrogen evolution. *Nat. Commun.* **2018**, *9*, 1460. [CrossRef]
95. Zheng, Z.; Xue, Y.; Li, Y. A new carbon allotrope: Graphdiyne. *Trends Chem.* **2022**, *4*, 754–768. [CrossRef]
96. Yang, Z.; Li, Y.; Zhang, X.; Cui, X.; He, S.; Liang, H.; Ding, A. Sludge activated carbon-based CoFe2O4-SAC nanocomposites used as heterogeneous catalysts for degrading antibiotic norfloxacin through activating peroxymonosulfate. *Chem. Eng. J.* **2020**, *384*, 123319. [CrossRef]
97. Gągol, M.; Przyjazny, A.; Boczkaj, G. Wastewater treatment by means of advanced oxidation processes based on cavitation—A review. *Chem. Eng. J.* **2018**, *338*, 599–627. [CrossRef]
98. Boczkaj, G.; Gągol, M.; Klein, M.; Przyjazny, A. Effective method of treatment of effluents from production of bitumens under basic pH conditions using hydrodynamic cavitation aided by external oxidants. *Ultrason. Sonochem.* **2018**, *40*, 969–979. [CrossRef] [PubMed]
99. Gągol, M.; Przyjazny, A.; Boczkaj, G. Highly effective degradation of selected groups of organic compounds by cavitation based AOPs under basic pH conditions. *Ultrason. Sonochem.* **2018**, *45*, 257–266. [CrossRef]
100. Gągol, M.; Soltani, R.D.C.; Przyjazny, A.; Boczkaj, G. Effective degradation of sulfide ions and organic sulfides in cavitation-based advanced oxidation processes (AOPs). *Ultrason. Sonochem.* **2019**, *58*, 104610. [CrossRef]
101. Rayaroth, M.P.; Aravind, U.K.; Aravindakumar, C.T. Degradation of pharmaceuticals by ultrasound-based advanced oxidation process. *Environ. Chem. Lett.* **2016**, *14*, 259–290. [CrossRef]
102. Fedorov, K.; Dinesh, K.; Sun, X.; Soltani, R.D.C.; Wang, Z.; Sonawane, S.; Boczkaj, G. Synergistic effects of hybrid advanced oxidation processes (AOPs) based on hydrodynamic cavitation phenomenon—A review. *Chem. Eng. J.* **2022**, *432*, 134191. [CrossRef]
103. Rayaroth, M.P.; Aravind, U.K.; Aravindakumar, C.T. Ultrasound based AOP for emerging pollutants: From degradation to mechanism. *Environ. Sci. Pollut. Res.* **2017**, *24*, 6261–6269. [CrossRef]
104. Philip, J.M.; Koshy, C.M.; Aravind, U.K.; Aravindakumar, C.T. Sonochemical degradation of DEET in aqueous medium: Complex by-products from synergistic effect of sono-Fenton—New insights from a HRMS study. *J. Environ. Chem. Eng.* **2022**, *10*, 107509. [CrossRef]
105. Lu, X.; Zhao, J.; Wang, Q.; Wang, D.; Xu, H.; Ma, J.; Qiu, W.; Hu, T. Sonolytic degradation of bisphenol S: Effect of dissolved oxygen and peroxydisulfate, oxidation products and acute toxicity. *Water Res.* **2019**, *165*, 114969. [CrossRef] [PubMed]
106. Chiha, M.; Hamdaoui, O.; Baup, S.; Gondrexon, N. Sonolytic degradation of endocrine disrupting chemical 4-cumylphenol in water. *Ultrason. Sonochem.* **2011**, *18*, 943–950. [CrossRef] [PubMed]
107. Chu, J.-H.; Kang, J.-K.; Park, S.-J.; Lee, C.-G. Bisphenol A degradation using waste antivirus copper film with enhanced sono-Fenton-like catalytic oxidation. *Chemosphere* **2021**, *276*, 130218. [CrossRef]
108. Byrne, C.; Subramanian, G.; Pillai, S.C. Recent advances in photocatalysis for environmental applications. *J. Environ. Chem. Eng.* **2018**, *6*, 3531–3555. [CrossRef]
109. Banerjee, S.; Pillai, S.C.; Falaras, P.; O'shea, K.E.; Byrne, J.A.; Dionysiou, D.D. New Insights into the Mechanism of Visible Light Photocatalysis. *J. Phys. Chem. Lett.* **2014**, *5*, 2543–2554. [CrossRef]
110. Ye, T.; Qi, W.; An, X.; Liu, H.; Qu, J. Faceted TiO_2 photocatalytic degradation of anthraquinone in aquatic solution under solar irradiation. *Sci. Total. Environ.* **2019**, *688*, 592–599. [CrossRef]
111. Sirés, I.; Brillas, E.; Oturan, M.A.; Rodrigo, M.A.; Panizza, M. Electrochemical Advanced Oxidation Processes: Today and Tomorrow. A Review. *Environ. Sci. Pollut. Res.* **2014**, *21*, 8336–8367. [CrossRef]
112. Brillas, E.; Sirés, I.; Oturan, M.A. Electro-Fenton Process and Related Electrochemical Technologies Based on Fenton's Reaction Chemistry. *Chem. Rev.* **2009**, *109*, 6570–6631. [CrossRef]
113. Ganiyu, S.O.; Martínez-Huitle, C.A.; Oturan, M.A. Electrochemical advanced oxidation processes for wastewater treatment: Advances in formation and detection of reactive species and mechanisms. *Curr. Opin. Electrochem.* **2021**, *27*, 100678. [CrossRef]
114. Brito, L.R.; Ganiyu, S.O.; dos Santos, E.V.; Oturan, M.A.; Martínez-Huitle, C.A. Removal of antibiotic rifampicin from aqueous media by advanced electrochemical oxidation: Role of electrode materials, electrolytes and real water matrices. *Electrochim. Acta* **2021**, *396*, 139254. [CrossRef]
115. Wang, Q.; Lu, X.; Cao, Y.; Ma, J.; Jiang, J.; Bai, X.; Hu, T. Degradation of Bisphenol S by heat activated persulfate: Kinetics study, transformation pathways and influences of co-existing chemicals. *Chem. Eng. J.* **2017**, *328*, 236–245. [CrossRef]
116. Ren, W.; Huang, X.; Wang, L.; Liu, X.; Zhou, Z.; Wang, Y.; Lin, C.; He, M.; Ouyang, W. Degradation of simazine by heat-activated peroxydisulfate process: A coherent study on kinetics, radicals and models. *Chem. Eng. J.* **2021**, *426*, 131876. [CrossRef]

117. Ioannidi, A.; Arvaniti, O.S.; Nika, M.-C.; Aalizadeh, R.; Thomaidis, N.S.; Mantzavinos, D.; Frontistis, Z. Removal of drug losartan in environmental aquatic matrices by heat-activated persulfate: Kinetics, transformation products and synergistic effects. *Chemosphere* **2022**, *287*, 131952. [CrossRef]
118. Deng, J.; Shao, Y.; Gao, N.; Deng, Y.; Zhou, S.; Hu, X. Thermally activated persulfate (TAP) oxidation of antiepileptic drug carbamazepine in water. *Chem. Eng. J.* **2013**, *228*, 765–771. [CrossRef]
119. Lebik-Elhadi, H.; Frontistis, Z.; Ait-Amar, H.; Madjene, F.; Mantzavinos, D. Degradation of pesticide thiamethoxam by heat–activated and ultrasound—Activated persulfate: Effect of key operating parameters and the water matrix. *Process. Saf. Environ. Prot.* **2020**, *134*, 197–207. [CrossRef]
120. Sonawane, S.; Rayaroth, M.P.; Landge, V.K.; Fedorov, K.; Boczkaj, G. Thermally activated persulfate-based Advanced Oxidation Processes—Recent progress and challenges in mineralization of persistent organic chemicals: A review. *Curr. Opin. Chem. Eng.* **2022**, *37*, 100839. [CrossRef]
121. Liu, J.; Jiang, S.; Chen, D.; Dai, G.; Wei, D.; Shu, Y. Activation of persulfate with biochar for degradation of bisphenol A in soil. *Chem. Eng. J.* **2020**, *381*, 122637. [CrossRef]
122. Rayaroth, M.P.; Lee, C.-S.; Aravind, U.K.; Aravindakumar, C.T.; Chang, Y.-S. Oxidative degradation of benzoic acid using Fe 0-and sulfidized Fe 0-activated persulfate: A comparative study. *Chem. Eng. J.* **2017**, *315*, 426–436. [CrossRef]
123. Sasi, S.; Rayaroth, M.P.; Devadasan, D.; Aravind, U.K.; Aravindakumar, C.T. Influence of inorganic ions and selected emerging contaminants on the degradation of Methylparaben: A sonochemical approach. *J. Hazard. Mater.* **2015**, *300*, 202–209. [CrossRef]
124. Guzman-Duque, F.; Pétrier, C.; Pulgarin, C.; Peñuela, G.; Torres-Palma, R.A. Effects of sonochemical parameters and inorganic ions during the sonochemical degradation of crystal violet in water. *Ultrason. Sonochem.* **2011**, *18*, 440–446. [CrossRef]
125. Serna-Galvis, E.A.; Silva-Agredo, J.; Giraldo-Aguirre, A.L.; Flórez-Acosta, O.A.; Torres-Palma, R.A. High frequency ultrasound as a selective advanced oxidation process to remove penicillinic antibiotics and eliminate its antimicrobial activity from water. *Ultrason. Sonochem.* **2016**, *31*, 276–283. [CrossRef] [PubMed]
126. Nikolaou, S.; Vakros, J.; Diamadopoulos, E.; Mantzavinos, D. Sonochemical degradation of propylparaben in the presence of agro-industrial biochar. *J. Environ. Chem. Eng.* **2020**, *8*, 104010. [CrossRef]
127. Domínguez, J.R.; González, T.; Correia, S.; Domínguez, E.M. Sonochemical degradation of neonicotinoid pesticides in natural surface waters. Influence of operational and environmental conditions. *Environ. Res.* **2021**, *197*, 111021. [CrossRef] [PubMed]
128. Tan, C.; Gao, N.; Deng, Y.; Zhang, Y.; Sui, M.; Deng, J.; Zhou, S. Degradation of antipyrine by UV, UV/H2O2 and UV/PS. *J. Hazard. Mater.* **2013**, *260*, 1008–1016. [CrossRef]
129. Starling, M.C.V.; Souza, P.P.; Le Person, A.; Amorim, C.C.; Criquet, J. Intensification of UV-C treatment to remove emerging contaminants by UV-C/H2O2 and UV-C/S2O82−: Susceptibility to photolysis and investigation of acute toxicity. *Chem. Eng. J.* **2019**, *376*, 120856. [CrossRef]
130. Yang, Y.; Cao, Y.; Jiang, J.; Lu, X.; Ma, J.; Pang, S.; Li, J.; Liu, Y.; Zhou, Y.; Guan, C. Comparative study on degradation of propranolol and formation of oxidation products by UV/H2O2 and UV/persulfate (PDS). *Water Res.* **2019**, *149*, 543–552. [CrossRef]
131. Ghanbari, F.; Yaghoot-Nezhad, A.; Wacławek, S.; Lin, K.-Y.A.; Rodríguez-Chueca, J.; Mehdipour, F. Comparative investigation of acetaminophen degradation in aqueous solution by UV/Chlorine and UV/H2O2 processes: Kinetics and toxicity assessment, process feasibility and products identification. *Chemosphere* **2021**, *285*, 131455. [CrossRef]
132. Al-Hasani, H.; Al-Sabahi, J.; Al-Ghafri, B.; Al-Hajri, R.; Al-Abri, M. Effect of water quality in photocatalytic degradation of phenol using zinc oxide nanorods under visible light irradiation. *J. Water Process. Eng.* **2022**, *49*, 103121. [CrossRef]
133. Fard, M.A.; Aminzadeh, B.; Vahidi, H. Degradation of petroleum aromatic hydrocarbons using TiO_2 nanopowder film. *Environ. Technol.* **2013**, *34*, 1183–1190. [CrossRef]
134. Lair, A.; Ferronato, C.; Chovelon, J.-M.; Herrmann, J.-M. Naphthalene degradation in water by heterogeneous photocatalysis: An investigation of the influence of inorganic anions. *J. Photochem. Photobiol. A Chem.* **2008**, *193*, 193–203. [CrossRef]
135. Kashif, N.; Ouyang, F. Parameters effect on heterogeneous photocatalysed degradation of phenol in aqueous dispersion of TiO_2. *J. Environ. Sci.* **2009**, *21*, 527–533. [CrossRef] [PubMed]
136. Petala, A.; Frontistis, Z.; Antonopoulou, M.; Konstantinou, I.; Kondarides, D.I.; Mantzavinos, D. Kinetics of ethyl paraben degradation by simulated solar radiation in the presence of N-doped TiO_2 catalysts. *Water Res.* **2015**, *81*, 157–166. [CrossRef]
137. Jojoa-Sierra, S.D.; Silva-Agredo, J.; Herrera-Calderon, E.; Torres-Palma, R.A. Elimination of the antibiotic norfloxacin in municipal wastewater, urine and seawater by electrochemical oxidation on IrO2 anodes. *Sci. Total. Environ.* **2017**, *575*, 1228–1238. [CrossRef] [PubMed]
138. Barazesh, J.M.; Prasse, C.; Sedlak, D.L. Electrochemical Transformation of Trace Organic Contaminants in the Presence of Halide and Carbonate Ions. *Environ. Sci. Technol.* **2016**, *50*, 10143–10152. [CrossRef]
139. Lan, Y.; Coetsier, C.; Causserand, C.; Serrano, K.G. On the role of salts for the treatment of wastewaters containing pharmaceuticals by electrochemical oxidation using a boron doped diamond anode. *Electrochim. Acta* **2017**, *231*, 309–318. [CrossRef]